Site NGHP-01-09

By T. Collett, M. Riedel, J. Cochran, R. Boswell, J. Presley, P. Kumar, A. Sathe,
A. Sethi, M. Lall, and the National Gas Hydrate Program Expedition 01 Scientists

Scientific Investigations Report 2012–5054

U.S. Department of the Interior
U.S. Geological Survey

Contents

Figures

Site NGHP-01-09

By T. Collett, M. Riedel, J. Cochran, R. Boswell, J. Presley, P. Kumar, A. Sathe, A. Sethi, M. Lall, and the National Gas Hydrate Program Expedition 01 Scientists

Background and Objectives

Site NGHP-01-09 (Prospectus Site MNGH-01-2) is located at 18° 46.0897' N, 085° 37.502' E in the Mahanadi (MN) Basin (fig. 1). The water depth is ~1,935 m. The site is located within the Reliance Industry Ltd. D10 block with full 3D seismic coverage. Operations at this site are restricted to a total depth of 350 mbsf. This site was not selected as a primary coring site after the LWD/MWD campaign was completed.

The objectives of the work carried out at this site follow the general objectives of the India NGHP Expedition 01, with a focus on LWD/MWD operations only:

- Study the occurrence of gas hydrate and establish the background geophysical baselines for gas-hydrate studies;
- Define the relationship between the sedimentology and structure of the sediments and the occurrence and concentration of gas hydrate;
- Calibrate remote sensing data such as seismic data by acquiring LWD/MWD data;

The seismic data provided for this site (inline 3014) were extracted from a 3D cube (figs. 2 and 3). The sediments around this site are highly faulted, which contrasts with Site NGHP-01-08 in the eastern part of the Mahanadi Basin. The faults extend from the base of the imaged section to near the seafloor. A layer about 75 m below seafloor (mbsf) at Site NGHP-01-09 appears to be the upper limit of the fault system.

No clear bottom-simulating reflector (BSR) can be identified; however, at a depth of ~290 mbsf unusually high seismic reflectivity is identified, which could mark the occurrence of free gas associated with gas hydrate above. This zone of high reflectivity is also cut by the faults and does not form a continuous, cross-cutting reflection. Therefore uncertainty remains in the interpretation of this reflection being a BSR in this area.

Operations

This operations summary covers the transit from Site NGHP-01-08 (MNGH01-1-A) to Site NGHP-01-09 (MNGH01-2) and LWD/MWD drilling operations in Hole NGHP-01-09A (fig. 4). Schedule details and statistics for this site can be found as Appendixes:

- Appendix 1: NGHP Expedition 01 Operations Schedules
- Appendix 2: NGHP Expedition 01 Operations Statistics

Included in the "Methods" chapter and the glossary is a list of standard or commonly used operations terms and acronyms.

Hole NGHP-01-09A

The first and only hole of Site NGHP-01-09 was drilled on Leg 2 of NGHP Expedition 01 as the ninth hole of a twelve-hole LWD/MWD transect. The 12.6 NMI transit from Site NGHP-01-08 to Site NGHP-01-09 was completed in 1.7 hr at an average speed of 7.4 kt.

The sea voyage ended at 2300 hr May 30, 2006, and once thrusters were down, the vessel was switched over to DP control. A positioning beacon was deployed at the Hole NGHP-01-09A location coordinates at 0025 hr on May 31, 2006. The LWD/MWD tools, consisting of the GeoVISION (RAB), EcoScope, SonicVISION, and TeleScope, were assembled. The LWD/MWD tools were lowered to 91 mbrf and a flow test was conducted. The drill string was then lowered to the seafloor and spaced out for spudding. A tag of the seafloor indicated a mudline depth of 1,946.0 mbrf. For reference, the PDR depth at this site, adjusted to the rig floor DES, was 1,950.4 mbrf. After offsetting the vessel two meters N of the site coordinates, Hole NGHP-01-09A was spudded at 0604 hr on May 31. LWD/MWD drilling continued at a controlled rate of 22.8 m/h (or 18.6 m/h average net ROP including connection time) to a total depth of 330.0 mbsf. The hole was displaced with 103 barrels of 10.5 ppg mud, the top drive was set back, and the drill string was pulled clear of the seafloor at 0205 hr on June 1, 2006. After removing the nuclear source and downloading data, the LWD/MWD BHA was racked

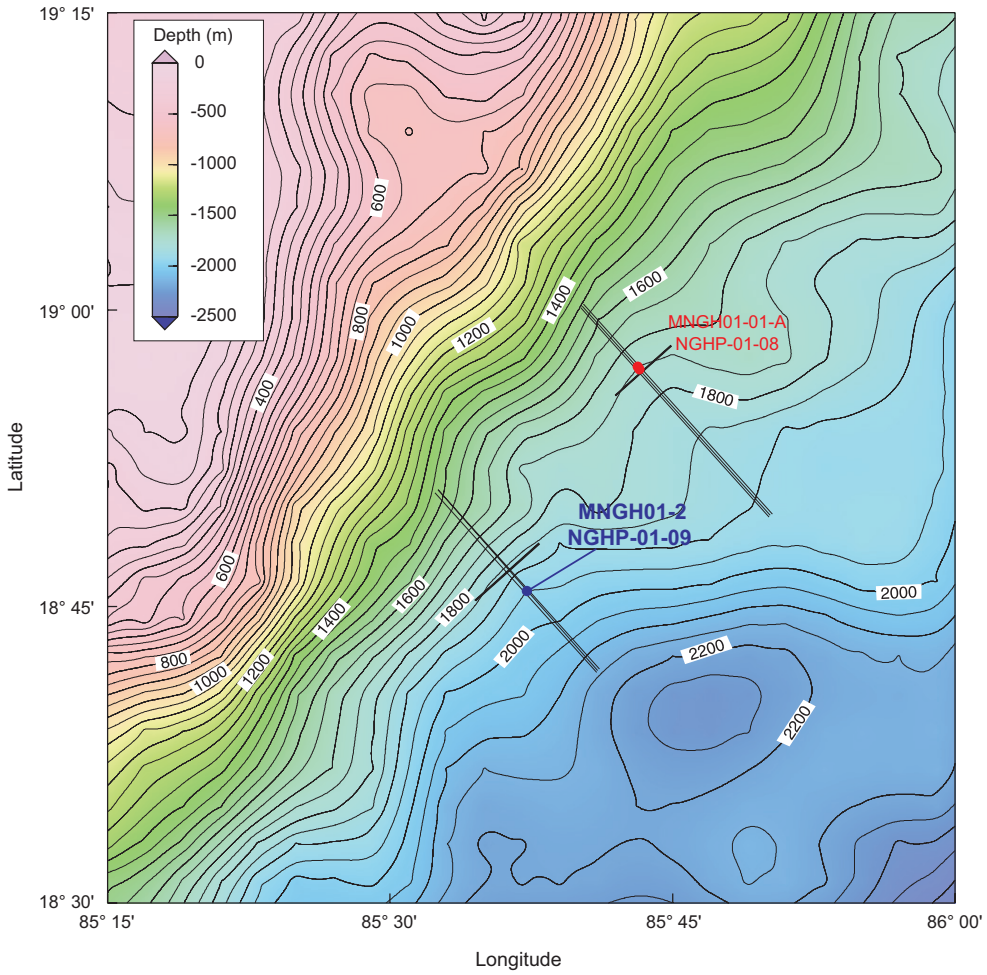

Figure 1. Location of Site NGHP-01-09 (Prospectus Site MNGH01-2) in the Mahanadi (MN) Basin.

back in the derrick. The rig was secured for transit, the beacon recovered, and the vessel got underway for Site NGHP-01-10 (GD-3-1) at 0710 hr on June 1, 2006. This completed operations at Site NGHP-01-09.

Downhole Logging

Logging While Drilling

Operations

After tagging the seafloor at 1,946 mbrf (driller's depth), Hole NGHP-01-09A was spudded at 0604 hr on May 31, 2006. LWD tools in the BHA included the GeoVISION, the EcoScope, the SonicVISION, and the TeleScope MWD tool. For details on LWD tool and measurement, see the "Downhole Logging" section in the "Methods" chapter.

To avoid washing out the formation near the seafloor, Hole NGHP-01-09A was spudded at a relatively low flow rate. The first 10 m were drilled at 100 gallons per minute (gpm) with a rotation rate of 20 rotations per minute (rpm) and a rate of penetration (ROP) of 25 m/h. Below 10 mbsf, the rotation rate was increased to 30 rpm; at 30 mbsf, it was increased to 60 rpm and the flow rate was increased to ~370 gpm until the LWD tools turned on, while keeping a constant ROP of 25 m/h. The target depth of 330 mbsf (2,276 mbrf) was reached at 0015 hr on June 1, 2006. After the complete drill string was pulled to the surface, data download and rig down were completed at 0710 hr on June 1.

Gas Monitoring with Real Time LWD/MWD Data

The LWD logs were acquired in the first hole drilled at Site NGHP-01-09 to plan coring and pressure coring operations in subsequent holes. As Hole NGHP-01-09A was drilled without coring, the LWD data had to be monitored for safety to detect gas entering the wellbore. As explained in the "Downhole Logging" section of the "Methods" chapter, the primary measurement used for gas monitoring was the "annular pressure while drilling" (APWD) measured by the EcoScope tool in the borehole annulus. We looked for sudden decreases of more than 100 psi in the annular pressure,

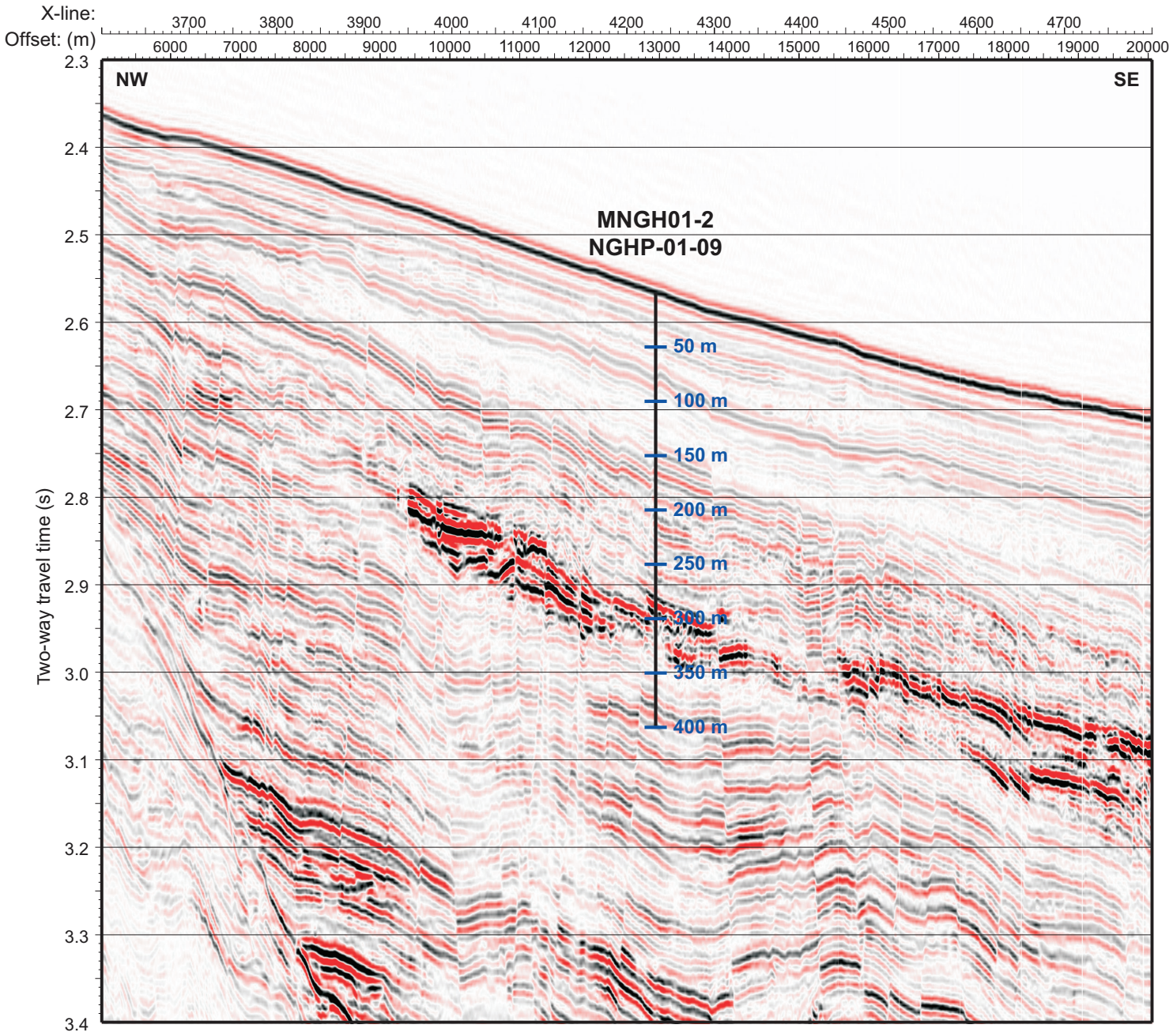

Figure 2. Section of seismic inline 3014 around Site NGHP-01-09 (Prospectus Site MNGH01-2) showing widespread faulting. No clear BSR can be identified. [BSR, bottom-simulating reflector]

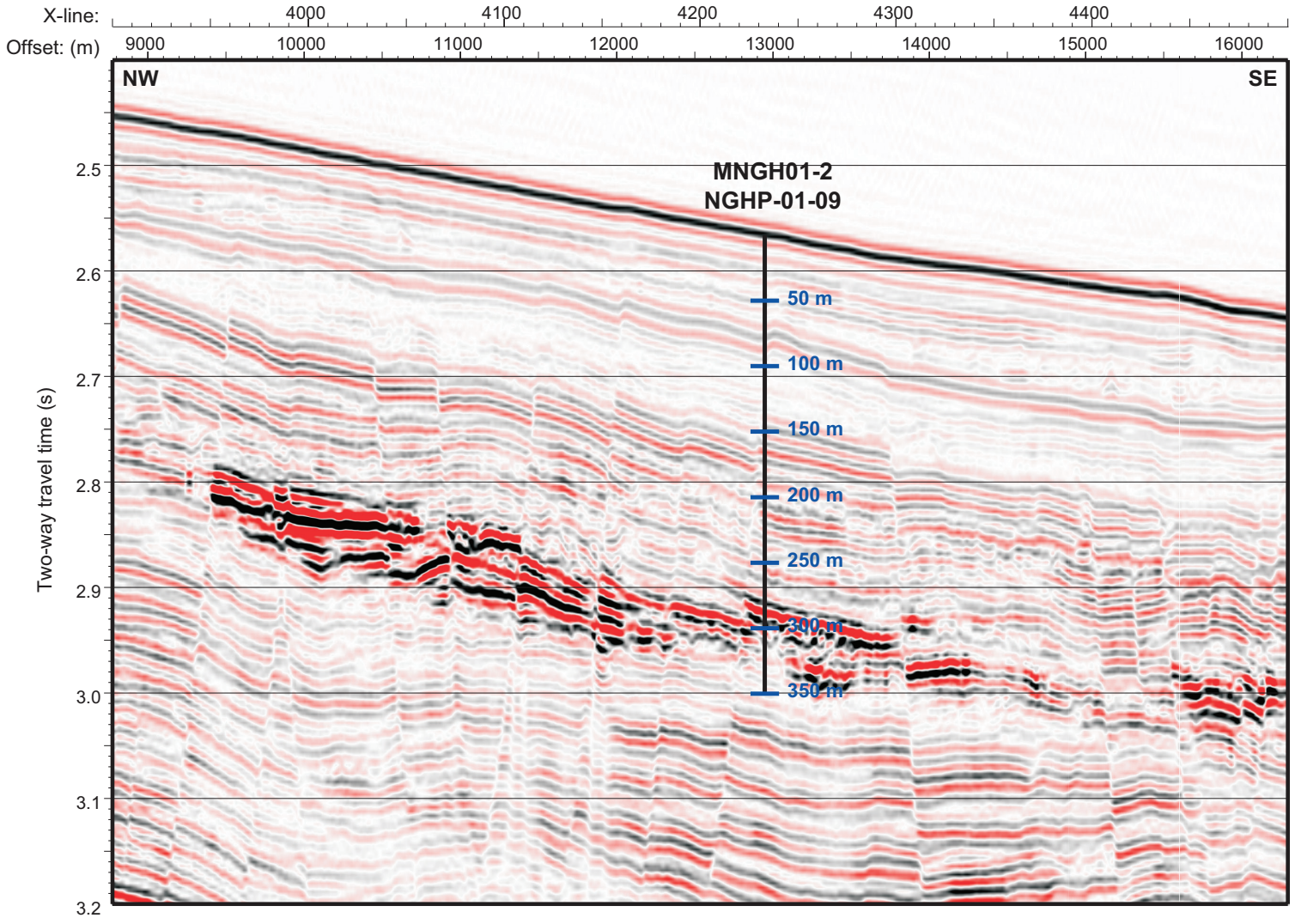

Figure 3. Close up of seismic inline 3014 around Site NGHP-01-09 (Prospectus Site MNGH01-2) with predicted formation depths based on a uniform seismic velocity of 1,610 m/s. [m/s, meters per second]

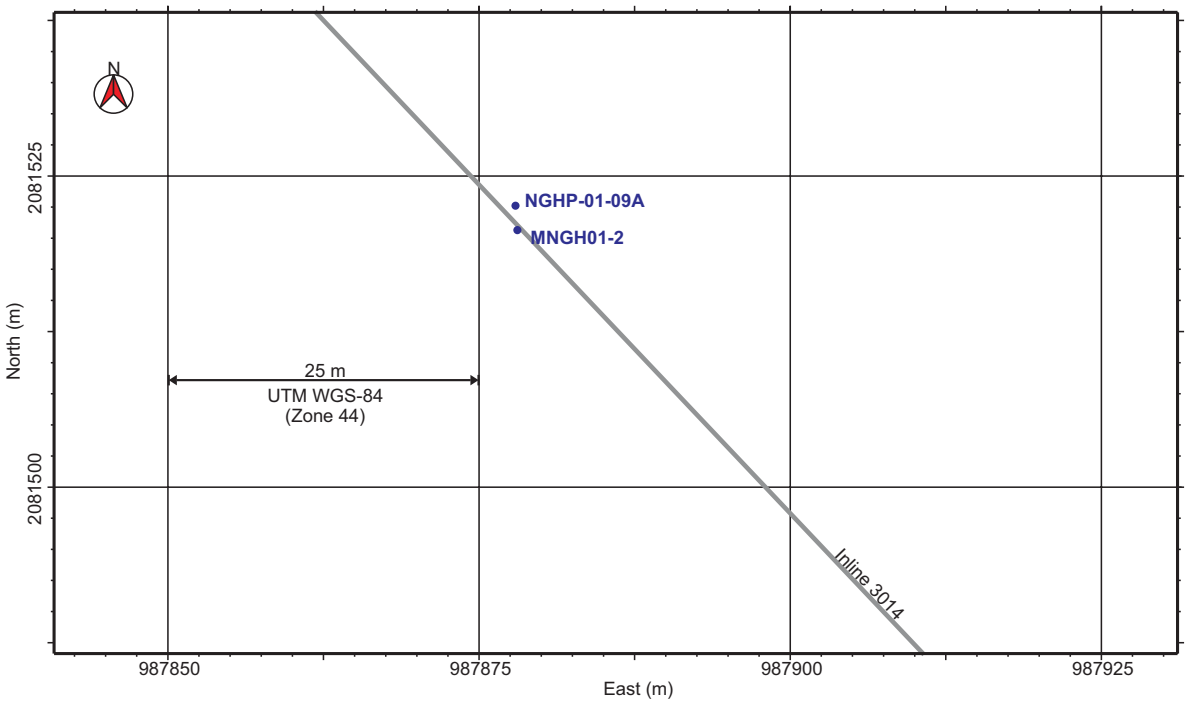

Figure 4. Map showing the hole occupied at Site NGHP-01-09 (MNGH01-2).

which could be due to low-density gas entering the wellbore. We also monitored pressure increases of the same magnitude, which could be due to fluid acceleration caused by a gas kick (Aldred and others, 1998).

Figure 5 shows the measured borehole fluid pressure in Hole NGHP-01-09A after subtraction of the hydrostatic pressure trend. This residual pressure curve shows only minor fluctuations that are well below the 100 psi level that would have required preventive action. We also monitored the coherence of the sonic waveforms acquired by the SonicVISION tool, which was configured to detect the borehole fluid wave arrival. Gas indicators are loss of coherence in the waveforms and decrease in fluid wave velocity, which were not observed throughout the interval drilled.

LWD Log Quality

Figure 5 also shows the quality control logs for Hole NGHP-01-09A. The two curves for rate of penetration are the instantaneous rate of penetration (ROP_RM) and the rate of penetration averaged over the last 5 feet (ROP5_RM). The occasional peaks in the instantaneous rate of penetration are artifacts due to depth fluctuations during pipe connections. The ROP is generally below 30 m/h, which is sufficient to record high-resolution GeoVISION resistivity images (for details, see "Downhole Logging" in the "Methods" chapter).

The density (DCAV) and ultrasonic caliper logs (UCAV) show an enlarged hole near the seafloor (30–100 mbsf), with a hole diameter up to 12 in. The bit size (dashed line in fig. 5) is 9 7/8 in, and the ultrasonic caliper shows that most of the borehole diameter below 100 mbsf is just above 10 in. The density caliper, however, shows a borehole smaller than the bit size for most of the interval below 80 mbsf; the ultrasonic caliper is a direct measurement of borehole size and is probably more reliable. The density correction, calculated from the difference between the short- and long-spaced density measurements, is everywhere within the interval 0–0.2 g/cm^3 (fig. 5), suggesting that the density measurements should be of good quality.

Figure 6 is a summary of the LWD gamma ray, density, neutron porosity, and resistivity logs measured in Hole NGHP-01-09A. The gamma ray and resistivity logs measured by the GeoVISION and the EcoScope generally agree. The GeoVISION and EcoScope gamma ray curves have the same shape, but are offset by about 20–30 gAPI; this difference is most likely due to tool calibration.

Figure 7 shows a comparison of the ring resistivity measured by the GeoVISION with the attenuation and phase resistivity curves obtained by the EcoScope tool at different frequencies and transmitter-receiver spacings. For a given transmitter-receiver spacing, the phase-shift EcoScope resistivities have higher vertical resolution than the attenuation resistivities and thus show more detail.

Figure 6 also shows two bulk density curves: RHOB is the average density measured by the EcoScope tool while rotating, while IDRO (image-derived density) is the value of density measured when the sensors were in closest contact with the formation. The two density curves are generally close, except for the interval 30–70 mbsf where the image-derived density is greater and likely more reliable.

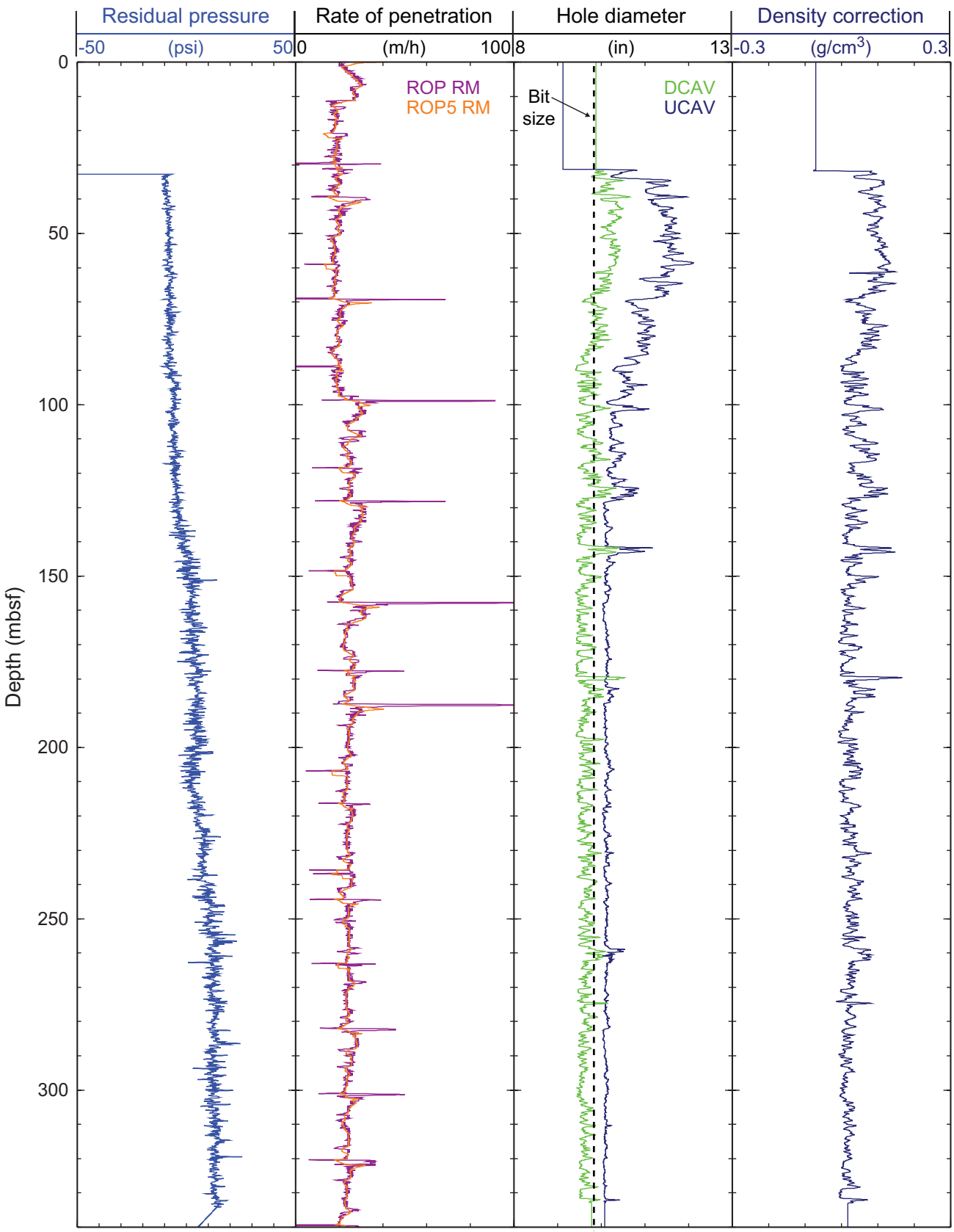

Figure 5. Monitoring and quality control LWD/MWD logs from Hole NGHP-01-06A. [LWD/MWD, logging-while-drilling/measuring-while-drilling; ROP_RM, Instantaneous rate of penetration; ROP5_RM, Rate of penetration averaged over a 5-ft interval; UCAV, Ultrasonic caliper; DCAV, density caliper]

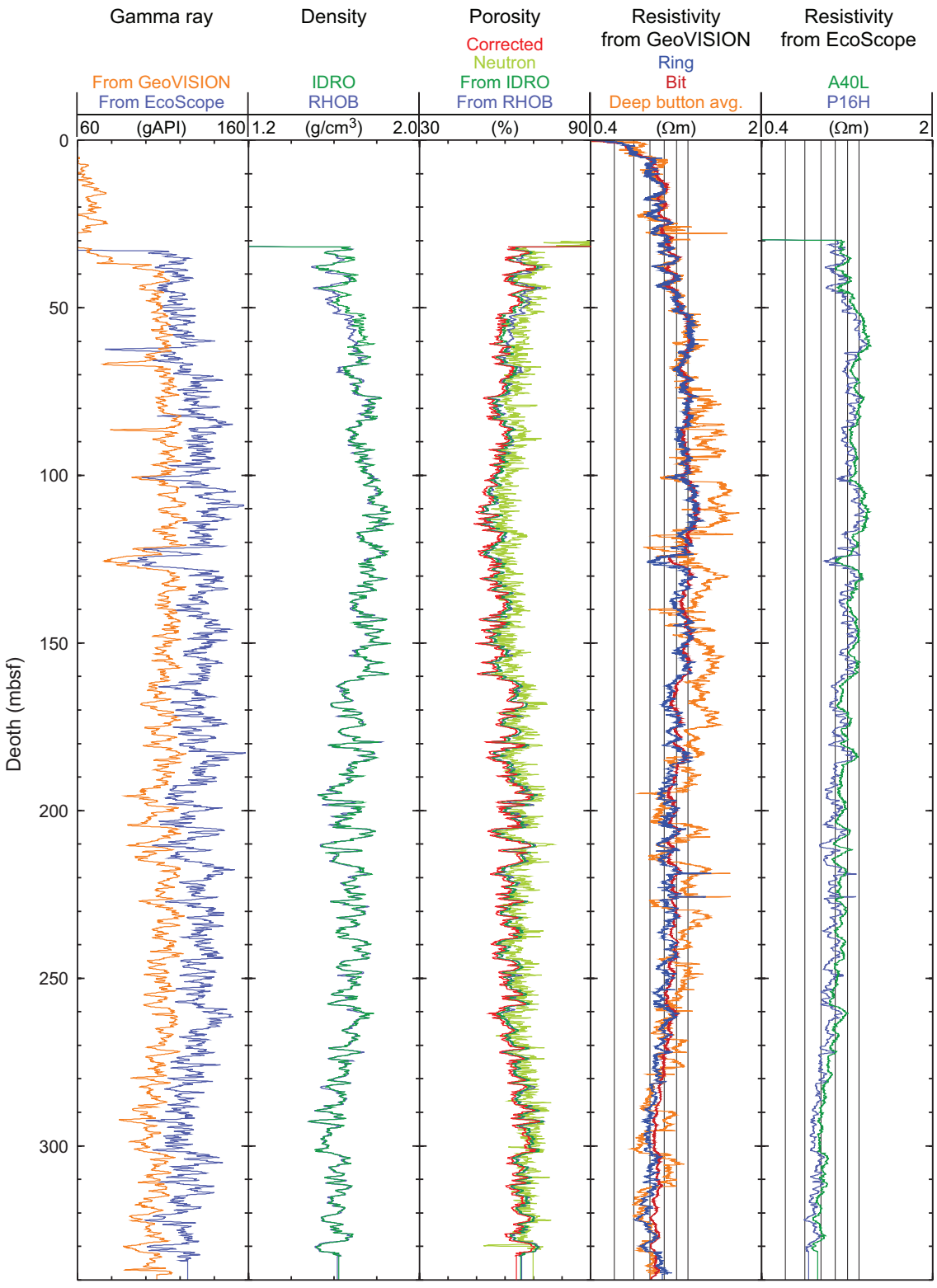

Figure 6. Summary of LWD log data from Hole NGHP-01-09A. [LWD, logging while drilling, gAPI, American Petroleum Institute gamma ray units; IDRO, Image-derived density (EcoScope); RHOB, Bulk density (EcoScope); neutron, Thermal neutron porosity (EcoScope); corrected density, density porosity with core derived grain densities (EcoScope); RING, Ring resistivity (GeoVISION); BIT, Bit resistivity (GeoVISION); Deep Button avg., Button deep resistivity (GeoVISION); A40L, Attenuation resistivity measured at 400 kHz and a transmitter-receiver spacing of 40 in (EcoScope); P16H, Phase-shift resistivity at 2 MHZ and a transmitter-receiver spacing of 16 in (EcoScope)]

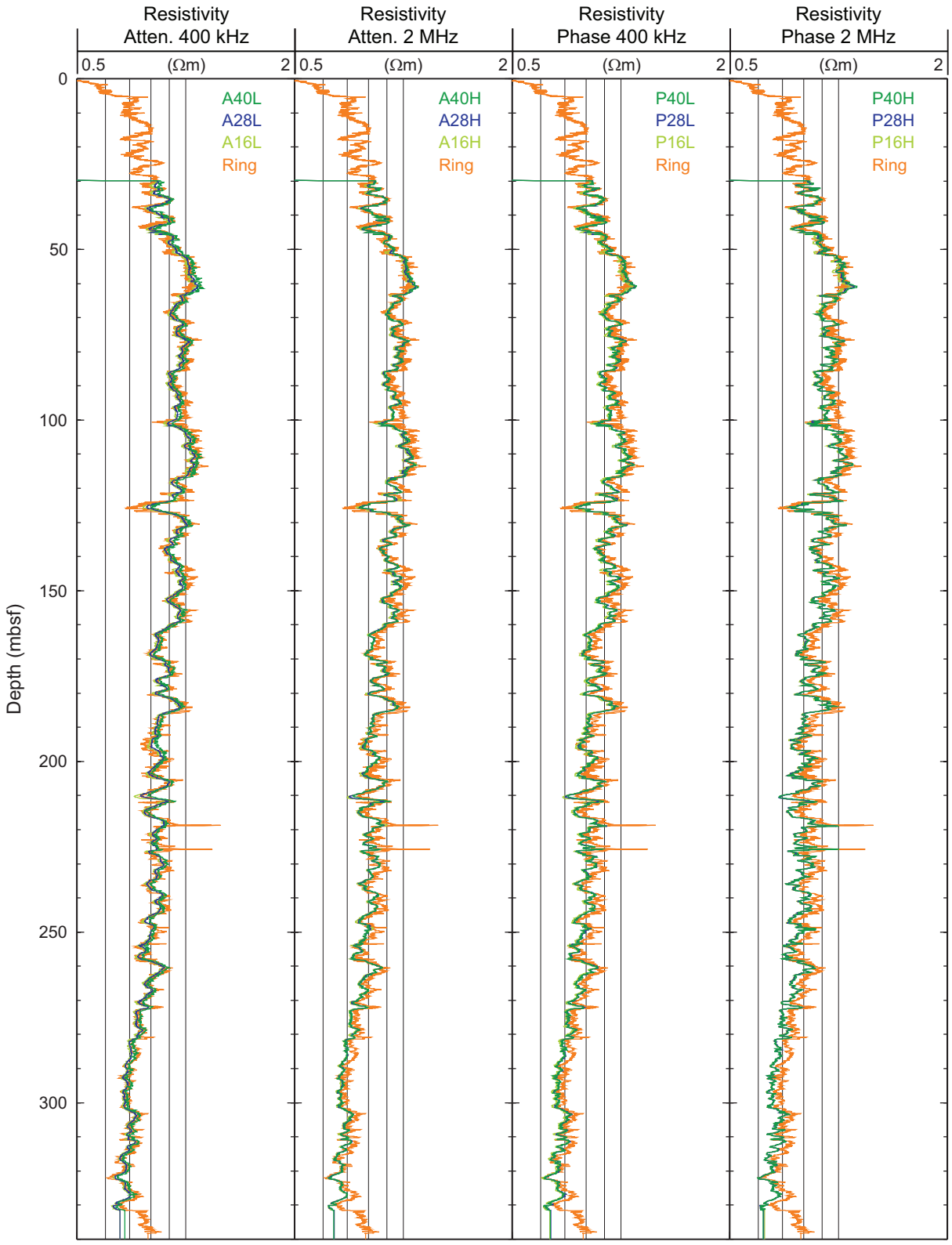

Figure 7. Comparison of LWD resistivity curves from Hole NGHP-01-09A. [LWD, logging while drilling; Ring, Ring resistivity (GeoVISION); AXXL, Attenuation resistivity measured at a frequency of 400 kHz, where XX is the transmitter-receiver spacing in inches (EcoScope); AXXH, Attenuation resistivity measured at a frequency of 2 MHz, where XX is the transmitter-receiver spacing in inches (EcoScope); PXXL, Phase-shift resistivity measured at a frequency of 400 kHz, where XX is the transmitter-receiver spacing in inches (EcoScope); PXXH, Phase-shift resistivity measured at a frequency of 2 MHz, where XX is the transmitter-receiver spacing in inches (EcoScope)]

The bottom-simulating reflector (BSR) that should mark the bottom of the gas-hydrate stability zone was estimated to be at a depth of 287 mbsf in this hole. There is no appreciable change in the LWD logs near this depth.

The depths relative to seafloor were fixed for all of the LWD logs by identifying the step change in the GeoVISION gamma ray log at the seafloor. For Hole NGHP-01-09A, the gamma ray logging pick for the seafloor was at a depth of 1,935 mbrf, 11 m shallower than the initial depth estimated by the drillers (1,946 mbrf). The rig floor logging datum was located 10.5 m above sea level.

LWD Porosities

Sediment porosities were calculated from the LWD density and neutron logs in Hole NGHP-01-09A. No core-derived physical property data were available at this site to calibrate and evaluate the log-derived porosities.

The LWD log-derived density measurements from Hole NGHP-01-09A were used to calculate sediment porosities (φ) with the standard density-porosity relation: $\varphi = (r_g - r_b) / (r_g - r_w)$. We used first a constant water density (r_w) of 1.03 g/cm^3 and a grain/matrix density (r_g) of 2.75 g/cm^3. The resulting density log-derived porosities from Hole NGHP-01-09A range from about 65 percent at 30 mbsf to about 55 percent around 150 mbsf (fig. 6). The density porosities in figure 6 were calculated from both the bulk density (RHOB) and from the image-derived density (IDRO).

To estimate the influence of variable grain density, but without any core sample measurements available at this site, we calculated a ”corrected porosity” from the IDRO density log and using a least square linear fit with depth of the grain density measurements made on samples from nearby Site NGHP-01-19. The results in figure 6 show only slightly lower porosity values than when assuming constant grain density.

The LWD neutron porosity log from Hole NGHP-01-09A (fig. 6) yielded sediment porosities ranging from an average value of about 70 percent at 30 mbsf to about 60 percent around 150 mbsf. Porosities measured by the neutron log are expected to be higher than those computed from the density log in clay-rich sediments, because the neutron log essentially quantifies hydrogen abundance, and counts hydrogen in clay minerals as porosity. The neutron porosity measured by the EcoScope tool shown in figure 6 is the “best thermal neutron porosity” (BPHI); it has been corrected so that the effect of clay is reduced (Adolph and others, 2005), and it is only marginally higher than the density porosity.

LWD Borehole Images

The GeoVISION and EcoScope LWD tools generate high-resolution images of borehole log data. The EcoScope tool produces images of density and hole radius (computed on the basis of the density correction, which depends on the borehole standoff). The GeoVISION produces a gamma ray image and resistivity images with shallow, medium and deep depth of investigation.

Figure 8 shows some of the LWD images collected by the EcoScope and GeoVISION tools. It should be noted that the display in figure 8 is highly compressed in the vertical direction. The unwrapped images are about 80 cm wide (for a 10 in diameter borehole) and the vertical scale is compressed relative to the horizontal by a factor of about 55:1. These high-resolution images can be used for detailed sedimentological and structural interpretations and to image gas-hydrate distribution in sediments (for example, in layers, nodules, fractures). Gas-hydrate-bearing sediments exhibit high resistivities within intervals of uniform or low bulk density. Layers with high resistivity and high density are likely to be low porosity, compacted, or carbonate-rich sediments. The two resistivity images in figure 8 correspond to two depths of investigation (for details, see “Downhole Logging” in the “Methods” chapter).

Gas hydrate-rich intervals show up in the LWD images as high resistivity intervals that do not correspond to matching high densities. There is no such indication of the presence of gas hydrate in the LWD images of figure 8.

Gas-Hydrate and Free Gas Occurrence

As previously discussed (see “Downhole Logging” in the “Methods” chapter), the occurrence of gas hydrate is generally identified by increases in electrical resistivity and acoustic velocity that are not accompanied by a corresponding porosity decrease. A decrease in porosity alone in water-saturated sediments can result in an increase in resistivity and acoustic velocity. Resistivities logs in Hole NGHP-01-09A show a general negative correlation with porosity (fig. 6), suggesting that little or no gas hydrate is present.

To make a quantitative estimate of the amount of gas hydrate at Site NGHP-01-09, we followed the procedure described in “Downhole Logging” in the “Methods” chapter, to apply the Archie relationship to the resistivity and porosity logs recorded in Hole NGHP-01-09A.

The procedure and the results are shown in figure 9. The pore fluid resistivity (R_w) was estimated from Fofonoff (1985) using a linear temperature profile derived from the *in situ* temperature measurements at nearby Site NGHP-01-19 (5 °C at the seafloor; gradient of 51 °C/km, see “Physical Properties” in the “Site NGHP-01-19” chapter) and a water salinity defined by the least square power law fit with depth of the values measured on pore water samples from Site NGHP-01-19. The estimated m curve is derived from R_w, the porosity (φ) and resistivity (R_t) logs ($m_{est} = -\log F / \log\varphi$, where $F = R_t / R_w$). As this relationship is defined for water-saturated sediments, the chosen value of $m = 2.1$ is given by the baseline of this curve in the low-resistivity intervals where there is likely no gas hydrate. Using the porosity log and Archie’s equation ($R_0 = (a\, R_w) / f^m$), we derive the predicted resistivity of the water-saturated formation R_o. A qualitative influence of

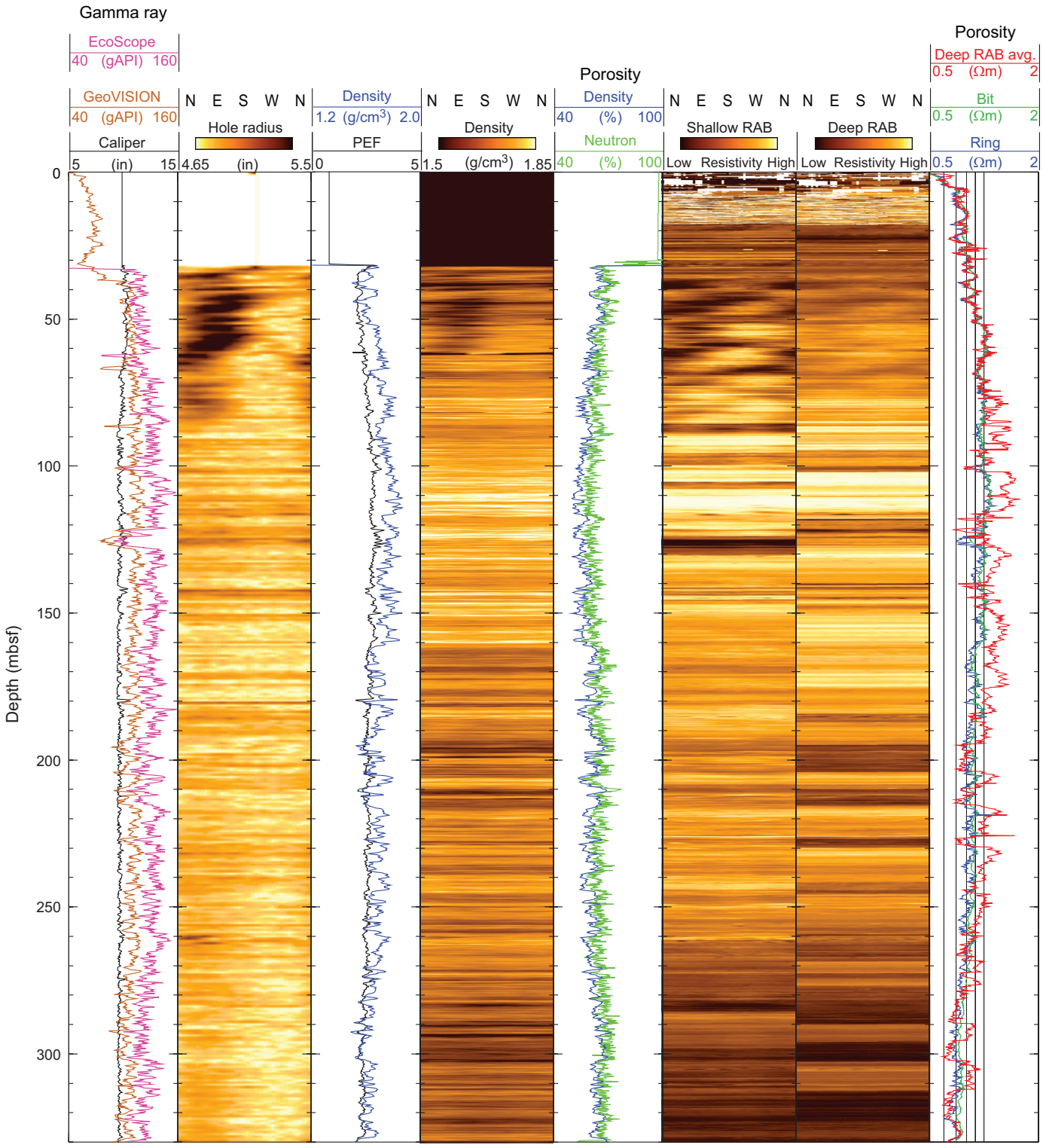

Figure 8. LWD image data from Hole NGHP-01-09A. [LWD, logging while drilling; gAPI, American Petroleum Institute gamma ray units; RAB, resistivity-at-bit image obtained by the GeoVISION tool]

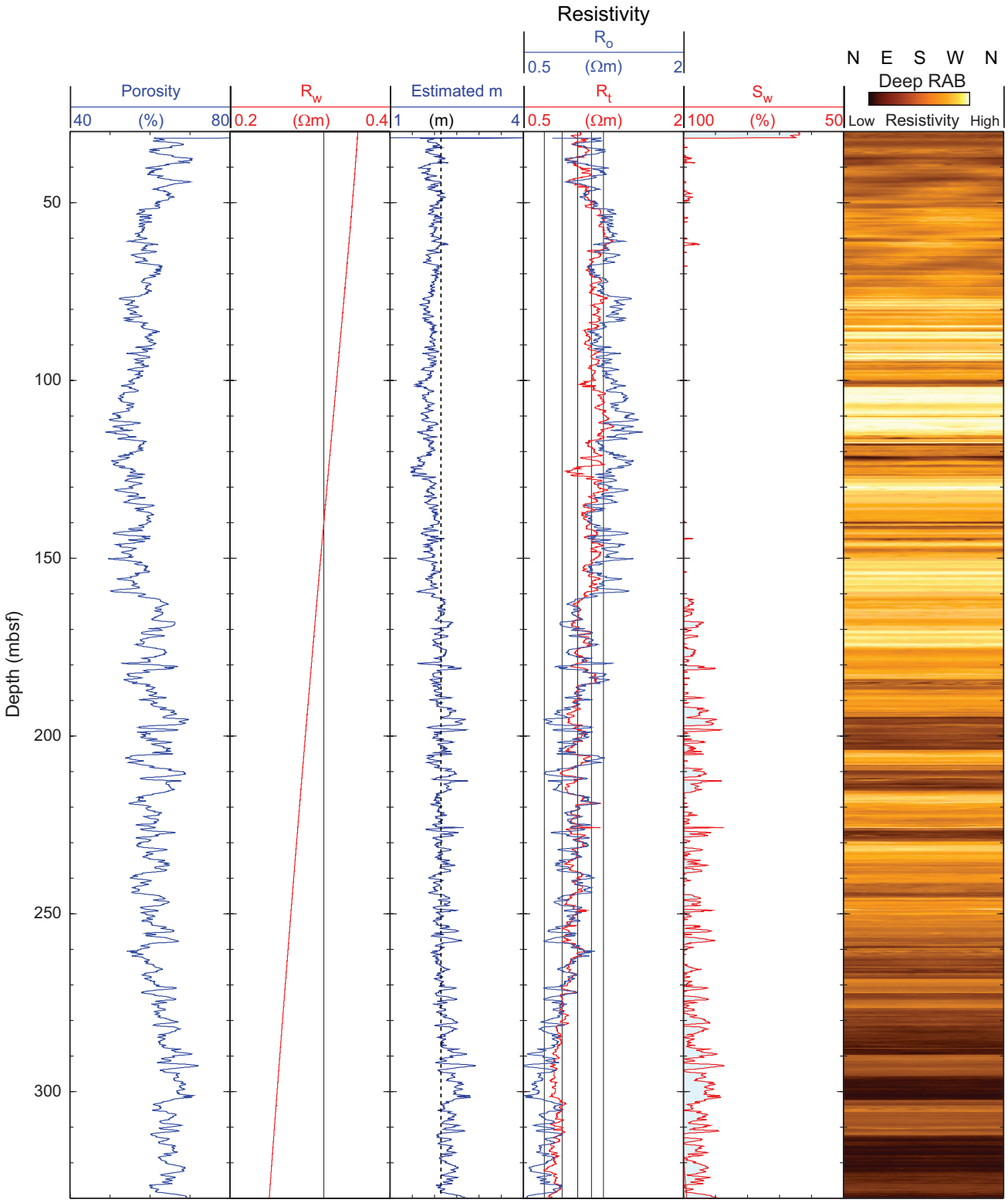

Figure 9. Water saturations from Archie's equation and LWD porosity and resistivity logs in Hole NGHP-01-09A. [LWD, logging while drilling; Rw, Formation water resistivity, R0, Computed formation resistivity for 100 percent water saturation; Rt, measured resistivity; Sw, water saturation]

gas hydrate on the resistivity log is indicated by the difference between the R_0 and the measured resistivity R_t. The estimated water saturation, assumed to be the numerical complement of the hydrate saturation, is $S_w = (R_0/R_t)^{1/n}$, where n=2 (Pearson and others, 1983). We used the "corrected" density porosity computed from the image-derived density (IDRO) and the resistivity from the 16 in, phase-shift, high-frequency propagation resistivity (P16H) measured by the EcoScope tool. We use the P16H curve because it is the resistivity with the highest vertical resolution measured by the EcoScope.

As noted earlier, the porosity and resistivity curves in Hole NGHP-01-09A generally mirror each other, so that the computed water-saturated resistivity R_0 is very close to the measured resistivity R_t and the water saturation S_w is close to 100 percent over most of the interval logged (fig. 9). However, below ~190 mbsf, the results suggest that as much as 10 percent of the pore space could be occupied either by gas hydrate above the BSR (estimated at ~287 mbsf, see "Background and Objectives"), or by free gas below.

References Cited

Adolph, B., Archer, M., Codazzi, D., el-Halawani, T., Perciot, P., Weller, G., Evans, M., Grant, J., Griffiths, R., Hartman, D., Sirkin, G., Ichikawa, M., Scott, G., Tribe, I., and White, D., 2005, No more waiting—Formation evaluation while drilling: Oilfield Review, Autumn 2005, p. 4–21.

Aldred, W., Cook, J., Bern, P., Carpenter, B., Hutchinson, M., Lovell, J., Rezmer-Cooper, I., and Leder, P.C., 1998, Using downhole annular pressure measurements to improve drilling performance: Oilfield Review, Winter 1998, p. 40–55.

Fofonoff, N.P., 1985, Physical properties of seawater: Journal of Geophysical Research, v. 90, no. C2, p. 3332–3342.

Pearson, C.F., Halleck, P.M., McGuire, P.L., Hermes, R., and Mathews, M., 1983, Natural gas hydrate deposits—A review of *in situ* properties: Journal of Physical Chemistry, v. 87, p. 4180–4185.